Modeling of deep indentation in brittle materials

Nathalie Olivi-Tran, Florence Despetis, Annelise Faivre

Modeling of deep indentation in brittle materials

Nathalie Olivi-Tran, Florence Despetis, Annelise Faivre

[1] *Universite Montpellier ,*

Laboratoire Charles Coulomb UMR 5221,

CC 074, place E.Bataillon,

F-34095, Montpellier, France

(Dated: February 18, 2020)

Abstract

We modelled deep indentation in brittle materials via a tensorial approach in three dimensions. Experimentally, we performed deep indentation in base catalyzed aerogels. When deep indentation is performed in these materials, it appears a Hertzian cone crack for both experimental and numerical results. The cone angle (angle between the surface and the boundaries of the Hertzian cone) depends on the material in which indentation is performed. The Young moduli of the materials has no effect on these angles. The tendency is that materials with increasing Poisson ratios have a decreasing value of the Hertzian cone angle.

I. INTRODUCTION

Hertz (Hertz 1881) was the first to observe what is now known as a Hertzian cone crack. Hertz performed deep indentation in a brittle material, a soda lime glass and observed a conical crack. More recently, Lawn (Lawn 1993) wrote a complete study of fracture in brittle solids.

Several experimental studies dealt with deep indentation and with the appearance of a Hertzian cone crack ((Chaudhri 2015,Chaudhri 1986) and references within). Experimentally, indentation is deep when the indentation depth is larger than $500\mu m$. There are two ways to obtain Hertzian cone crack in brittle materials: with an indenter (like the dentist uses) or with a particle impacting the brittle material.

In this article, we present results about deep indentation in silica aerogels. Deep indentation on base catalyzed silica aerogels has been performed with a flat punch indenter. Although mechanical characteristics of silica aerogels like their Young modulus, their Poisson ratio, their rupture threshold were already measured, there are few studies in which Hertzian cone angles were observed in these materials. Faivre et al.(Faivre 2018) recently published experimental results of deep indentation on different types of aerogels.

Up to now there are several simulations of deep indentation in brittle materials. Most of them modelled Hertzian cone cracks by using Finite Element Model and by assuming that the cone cracks follows the trajectory of the minimum principal stress, defined by the preexisting or evolving stress field (Lawn 1993,Warren 1978,Tumbajoy 2013,Kocer 1998,Zeng 1992a).

We use here a numerical tensorial approach to model deep indentation in brittle materials. This method leads to a Hertzian cone crack numerically. Contrarily to the models found in literature, we use no assumption considering the stress or strain fields in the materials. We obtain Hertzian cone cracks with angles depending on the Poisson ratios of the modelled materials.

We present, in section II, the experimental procedure that we used to obtain silica aerogels and straightforwardly the deep indentation experiments in these materials. In section III a numerical model based on tensors (strain and stress tensors) is detailed which leads to cone shaped cracks. In the last section (section IV), we compare the shape of the cracks obtained numerically and experimentally. The angles of the cone shaped cracks with respect

to the surface of the material and obtained numerically depend on the Poisson ratios and correspond within the error margin to the experimental values of these angles.

II. EXPERIMENTAL VALUES OF THE HERTZIAN CONE ANGLE: EXAMPLE OF AEROGELS

Silica aerogels were obtained from silica gels after supercritical drying of these gels (Brinker 1990). These silica gels were prepared using tetramethoxysililane (TMOS) diluted in ethanol. The hydrolysis and polycondensation reactions were performed under basic conditions($NH_4OH10^{-3}N$) to produce transparent aerogels (Pajonk 1998).

Deep indentation was performed in these silica aerogels using a universal testing machine (Instron 5500). This set up allowed us to measure the elastic modulus of the aerogels and the mechanical behavior under large penetration depths.

The applied load was measured with a loading cell with a maximum load of $2000g$.

The Young modulus was determined using the tip which was pressed at a constant tip displacement into the aerogel until a given maximum depth was reached (Faivre 2018). In this case, the depth used is a low depth indentation although it may reach $500\mu m$.

The following table 1 gives the measured Young modulus of different densities of aerogels (varying the TMOS/Ethanol ratio).

Following the review on the mechanical properties of aerogels by Woignier (Woignier 1998,Woignier 2017), the rupture threshold of these aerogels ranges from $0.01MPa$ to $2MPa$. Finally, the Poisson ratio ν is included between 0.18 and 0.21 for our aerogels which are brittle materials.

For deep indentation,the piercing displacement rate ranged from $1mm/min$ to $400mm/min$ using a tip with a cross section of $0.7mm$. In figure 1, you can see the Hertzian cone angles obtained after having performed deep indentation in base catalyzed silica aerogels. In table II, you may see the values of the Hertzian cone angle in aerogels.

III. NUMERICAL MODEL

We model deep indentation in brittle materials with a flat punch indenter. The indenter has a square cross section of $1A.U.$ (Arbitrary Units) edge length. We use a tensorial

approach to simulate the action of the indenter on the material. Our model differs from Finite Element Model and from Finite Difference Model so we do not have to put boundaries values in our model. The boundary values are intrinsic to our tensorial model.

In the case of an uniaxial stress along the z axis ,the strain tensor is :

$$\begin{pmatrix} \epsilon_{xx} & 0 & 0 \\ 0 & \epsilon_{yy} & 0 \\ 0 & 0 & \epsilon_{zz} \end{pmatrix} \tag{1}$$

The stress tensor T for a brittle material which is pierced without rotation of the indenter along z axis, writes :

$$\begin{pmatrix} 0 & 0 & 0 \\ 0 & 0 & 0 \\ 0 & 0 & \sigma_{zz} \end{pmatrix} \tag{2}$$

The material is an isotropic material thus the off-diagonal terms of the stress tensor are equal to zero. The material is a cube of edge length L, so the indenter pierces it vertically on location $x = L/2$, $y = L/2$ and $z = 0$ at time $t = 0$. The system of coordinates is chosen in order that the indenter applies its stress to a square $dxdy$ on the upper face of the material and in the middle of this face (see fig.1).

The initial internal stress of the material at time $t = 0$ is modelled by a 4 dimensions table which writes:

$$A(x, y, z, t = 0) = 0A.U. \tag{3}$$

$A(x, y, z, t)$ is a number which represents the stress within the material at location (x, y, z) and for time t.

We have:

$$\begin{aligned} \sigma_{xx} &= A(x-1, y, z, t) + A(x, y, z, t) + A(x+1, y, z, t) \\ \sigma_{yy} &= A(x, y-1, z, t) + A(x, y, z, t) + A(x, y+1, z, t) \\ \sigma_{zz} &= A(x, y, z-1, t) + A(x, y, z, t) + A(x, y, z+1, t) \end{aligned} \tag{4}$$

where σ_{xx}, σ_{yy} and σ_{zz} are the local stresses (i.e. stresses at location (x, y, z)). For each time step $\Delta t = 1s$ the indenter pierces the material along the z axis within Δz depth. So, table $A(x, y, z, t)$ represents the internal stresses within the material with one exception

$A(L/2, L/2, z, t)$ which is constant and larger than zero for $z = 1$ to $z = t$. This exception represents the indenter which pierces the material on a depth equal to $t.v$ where v is the piercing velocity (we set $v = 1\frac{\Delta z}{\Delta t}$)).

At time $t = 1s$ (first time step),

$$\sigma_{zz} = A(L/2, L/2, z = 1, t = 1s) \tag{5}$$

Indeed, at time=$0 + \Delta t = 1s$, only $A(x = L/2, y = L/2, z = 1, t = 0 + \Delta t = 1s) \neq 0$. Moreover, at time equal to $1s$, σ_{xx} and σ_{yy} are both equal to zero (see equation 2) because the stress is uniaxial.

For $x \neq L/2$ and $y \neq L/2$, the local stresses are no more uniaxial (indeed, the indenter applies a stress only at $x = L/2$ and $y = L/2$) , thus σ_{xx} and σ_{yy} are both different from zero. In order to conserve the rotational symmetry around the z axis (represented by the indenter) for the whole material, we calculate only the local stress σ_{zz} at time $t+\Delta t = t+1s$ as a function of σ_{zz}, of σ_{xx} and σ_{yy}, at time t.

Straightforwardly, at time $t > 1s$, the local stress σ_{zz} becomes

$$\sigma_{zz} = \sigma_{zz} + \nu(\sigma_{xx} + \sigma_{yy}) \tag{6}$$

where the right hand side of equation (6) correspond to time t and the left hand side to time $t + \Delta t$.

So equation 6 becomes:

$$\begin{aligned} A(x, y, z, t + 1) = (A(x, y, z - 1, t) + A(x, y, z + 1, t) + A(x, y, z, t)) \\ +\nu(A(x + 1, y, z, t) + A(x - 1, y, z, t) + 2A(x, y, z, t) \\ +A(x, y + 1, z, t) + A(x, y - 1, z, t)) \end{aligned} \tag{7}$$

We use equation 7 to compute the evolution of the internal stresses of the material. For each time step $t + \Delta t = t + 1$, the table $A(x, y, z, t + 1)$ is computed following equation 7, and represents the local stresses at location (x, y, z). If $A(x, y, z, t)$ is larger that the rupture threshold at time t, then $A(x, y, z, t + 1)$ is set to zero , this is the fracture criterion (except for the stress $A(L/2, L/2, z = 1$ to $v.t, t)$ which is larger than zero and constant). At each time step, the stresses are computed and correspond to a quasi static evolution.

We perform several computing with different mechanical parameters: the results do not depend on the Young modulus (see equations 6 and 7), but on the Poisson ratios $\nu = 0.15$ or $\nu = 0.20$ or $\nu = 0.25$ or $\nu = 0.30$ or $\nu = 0.33$.

IV. RESULTS AND DISCUSSION

In figure 2, we present Hertzian cone cracks for different aerogels in which we performed deep indentation. The aerogels had a density of $0.07, 0.1$ or 0.15, the piercing velocity was $v = 10mm/min$ or $100mm/min$.

The mean Poisson ratio for base catalyzed silica aerogels is equal to 0.20 (Woignier 1998,Woignier 2017). In table II, we present the values of the angle in degrees between the cone and the upper surface of the experimental samples (see figure 3). This angle ranges from 33.6 to 37.5^o.

In figures 4 and 5, we represent the stresses in the materials obtained with our numerical model. We used four different values of the Poisson ratios: 0.15, 0.20 , 0.25 or 0.30 and two values of the indentation depths (equal to $2A.U.$ or $8A.U.$). The numerical results did not depend on the Young moduli (see section III, equations 6 and 7). The residual stresses were represented following a cut in the y, z plane. The residual stresses are cone shaped and the width of these residual stresses depend on the indenting depth and on the rupture threshold: this width is larger for larger indenting depths and larger rupture thresholds . The stresses represented in black in figures 4 and 5 are the upper boundaries of the Hertzian cone crack; indeed, these stresses have the largest possible values without rupture. As the material is isotropic, the stresses in the x, z plane are identical to that in the y, z plane.

We measured the angle with respect to the upper surface of the cone shaped cracks obtained with our numerical model (see table III). Contrarily to most of the models of the Hertzian cone angles(Lawn 1974), we made no hypotheses concerning the preexisting stress fields. We checked that the rupture threshold and the stress due to the indenter did not change the values of the Hertzian cone angle. We also checked that the indentation depths did not change the values of the numerical Hertzian cone angles. These angles values depend on the Poisson ratio: when the Poisson ratio increases, the value of the cone angle decreases. Let us notice that it is not possible to simulate the indenting velocity with our numerical model, indeed the time step that we used has no physical signification. Plus, the numerical

results did not depend on the Young moduli and we can observe that it is also the case of aerogels with different densities and Young moduli (see table I and table II).

We make the hypothesis that the shape of the indenter (flat punch or spherical) has an effect only close to the surface of the fractured material. Indeed, next to the surface, the experimental cracks are curved (Chaudhri 2015,Chaudhri 1986,Zeng 1992a,Zeng 1992b); the vertical cut of the cone becomes rectilinear below an indenting depth larger than the diameter of the indenter.

Chaudhri (Chaudhri 2015,Chaudhri 1986) performed several experiments of the response to impact (by spherical particles) of different materials. Except the high velocities of the spherical particles, these experiments may be compared to deep indentation in brittle materials.

Experimentally, cone shaped cracks were observed for materials having a Poisson ratio equal to $\nu = 0.17$ (like fused silica). The cone angle for this material ranges from 21.5^o to 57.5^o (see table IV). depending on the velocity of the indenter (Chaudhri 2015,Chaudhri 1986).

For a Poisson ratio of 0.20 (which corresponds to base catalyzed silica aerogels in this article) the numerical cone angle has a mean value equal to 35^o. Taking account of the inaccuracy of the measures, we can see that the Hertzian cone angles for aerogels do not depend on the indenting velocity (see table II).

Chaudhri(Chaudhri 2015,Chaudhri 1986) found a Hertzian cone angle for Pyrex (borosilicate glass, $\nu = 0.22$) of 46.5^o (let us notice that Chaudhri measures the semi included angle of the cone i.e. 90^o minus the cone angle, see figure 3). The same authors found a cone angle of 26^o in Al_2O_3 corresponding to a Poisson ratio equal to 0.24.

For a Poisson ratio of 0.25 (which corresponds to soda lime glass and to Al_2O_3/SiC whisker composite), we find a numerical cone angle of 36 ± 3 which is close to the experimental values for Hertzian cone angle of $28-31^o$ in Al_2O_3/SiC whisker composite (Zeng 1992a,Zeng 1992b), but larger than the value of the cone angle in soda lime glasses (Hertz 1881). Indeed, literature reports that the Hertzian cone angle is equal to 22^o for soda lime glasses (table IV and (Hertz 1881,Lawn 1993)). If Poisson's ratio is $\nu = 0.33$, the angle obtained numerically in the literature (Warren 1978,Lawn 1993) is equal to 22^o; this value is the same as the value that we obtained with our numerical model (see table III).

We plotted the Hertzian cone angles as a function of the Poisson ratios in figure 6. The

tendency for increasing Poisson ratios is decreasing cone angles. This tendency happens as well as for experimental cone angles as for numerical cone angles. Concerning the experimental values of the cone angle found in literature, the authors did not necessarily take into account the effects of the indenting velocity on these angles.Straightforwardly, the experimental cone angles have large error bars when plotted in figure 6.

V. CONCLUSION

We modelled deep indentation in brittle materials with a tensorial numerical approach with no use of preexisting stress fields within the materials. The Hertzian cone which was obtained after indentation had an angle with respect to the surface which depends on the indented material (Poisson ratio). The experimental value of the cone angle in aerogels is coherent with our numerical model. Moreover, the numerical and experimental results for the cone angle in brittle materials have the same decreasing behavior as a function of the increasing Poisson ratios.

[1] Brinker J. and Scherer G.W.,(1990) *Sol-gel Science: the Physics and chemistry of sol-gel processing* Academic Press, Boston

[2] Chaudhri M. (2015) *Dynamic fracture of inorganic glasses by hard spherical and conical projectiles* Philosophical Transactions of The Royal Society A: Mathematical Physical and Engineering Sciences vol.373 pp.2038

[3] Chaudhri M.M.,Kurkjian C.R.,(1986) *Impact of Small Steel Spheres on the Surfaces of Normal and Anomalous Glasses* J. Am. Ceram. Soc., vol. 69 pp. 404-410

[4] Faivre A., Duffours L.,Colombel P.,Despetis F.,(2018) *Mechanical behaviour of aerogels and composite aerogels submitted to specific penetration tests* J.of Sol-Gel Science and Techn. vol. 88 no.1 doi: 10.1007/s10971-018-4845-1

[5] Hertz H. (1881),*Uber die Beruhrung fester elastischer Korper*, Journal fur die reine und angewandte. Mathematik vol.92, pp.156-171

[6] Kocer C. and Collins R.E.,(1998) *The angle of Hertzian cone cracks* J. Am. Ceram. Soc., vol.81 pp. 17361742

[7] Lawn B.,(1993) *Fracture of brittle solids* (second edition) Cambridge University Press, Cambridge

[8] Lawn B.R.,Wilshaw T.R., Hartley N.E.W.,(1974) *A computer simulation study of Hertzian cone crack growth* Int. J. Fract. vol. 10 pp. 1-16

[9] Pajonk G.M.,(1998) *Transparent silica aerogels* J.of Non-Cryst. Solids vol. 225 pp. 307-314

[10] Tumbajoy-Spinel D.Y., Feulvarch E., Bergheau J.M.,Kermouche G., (2013), *2D axisymmetric X-FEM modeling of the Hertzian cone crack system* C.R. Mecanique vol.341 pp.715-725

[11] Warren R.,(1978) *Measurement of the fracture properties of brittle solids by hertzian indentation* Acta Metall. vol. 26 pp.1759-1769

[12] Woignier T., Reynes J.,Alaoui A.H., Beurroies I., Phalippou J.,(1998) *Different kinds of structure in aerogels: relationships with the mechanical properties* J.Non-Cryst.Solids vol.241 pp.45-52

[13] Woignier T.,(2017) Techniques de l'ingenieur, *Aerogels-Aspects Materiaux*

[14] Zeng K., Breder K. and Rowcliffe D. J., (1992) *The Hertzian stress field and formation of cone cracksI. Theoretical approach* Acta Metall. Mater. Vol. 40, No. 10, pp. 2595-2600

[15] Zeng K., Breder K. and Rowcliffe D. J., (1992) *The Hertzian stress field and formation of cone cracksII. Determination of fracture toughness* Acta Metall. Mater. Vol. 40, No. 10, pp. 2601-2605

ratio (%) TMOS/EtOH	ρ (g/cm^3)	Young modulus $E(MPa)$ (flat punch)
15	0.065 ±0.002	0.2 ±0.02
15	0.070 ±0.002	0.4 ±0.02
25	0.110 ±0.002	1.6 ±0.2
40	0.122 ±0.002	1.3±0.3
50	0.132 ±0.002	1.8 ±0.2

TABLE I. Densities and Young moduli for different silica base catalyzed aerogels

indentation velocity (mm/min)	indentation depth (mm)	Cone angle $(^o)$with respect to the surface
1	5	34.9 ±3
10	5	34.5 ±3
100	5	37.5 ±3
400	7	33.6 ±3

TABLE II. Cone angle in aerogels for different experimental indentation velocities and depths

ν Poisson ratio	Cone angle
0.15	$55^o \pm 5$
0.20	$44^o \pm 4$
0.25	$36^o \pm 3$
0.30	$28^o \pm 2$
0.33	$22^o \pm 2$

TABLE III. Cone angle for different numerical samples (depending on the Poisson ratio ν)

Material	ν Poisson ratio	Cone angle (^{o})
fused silica	0.17	21.5-57.5$^o \pm 5$ (Chaudhri 2015,Chaudhri 1986)
base catalyzed aerogels	0.20	35 $^o \pm 3$
borosilicate glass (Pyrex)	0.22	46.5 $^o \pm 5$(Chaudhri 2015,Chaudhri 1986)
Al_2O_3	0.24	26$^o \pm 3$ (Zeng 1992a,Zeng 1992b)
Al_2O_3/SiC whisker composite	0.25	28-31$^o \pm 3$ (Zeng 1992a,Zeng 1992b)
soda lime glass	0.25	22$^o \pm 2$ (Hertz 1881)
borate glass	0.29	no cone to 20$^o \pm 2$ (Chaudhri 2015,Chaudhri 1986)

TABLE IV. Cone angle for different experimental samples (depending on the Poisson ratio ν)

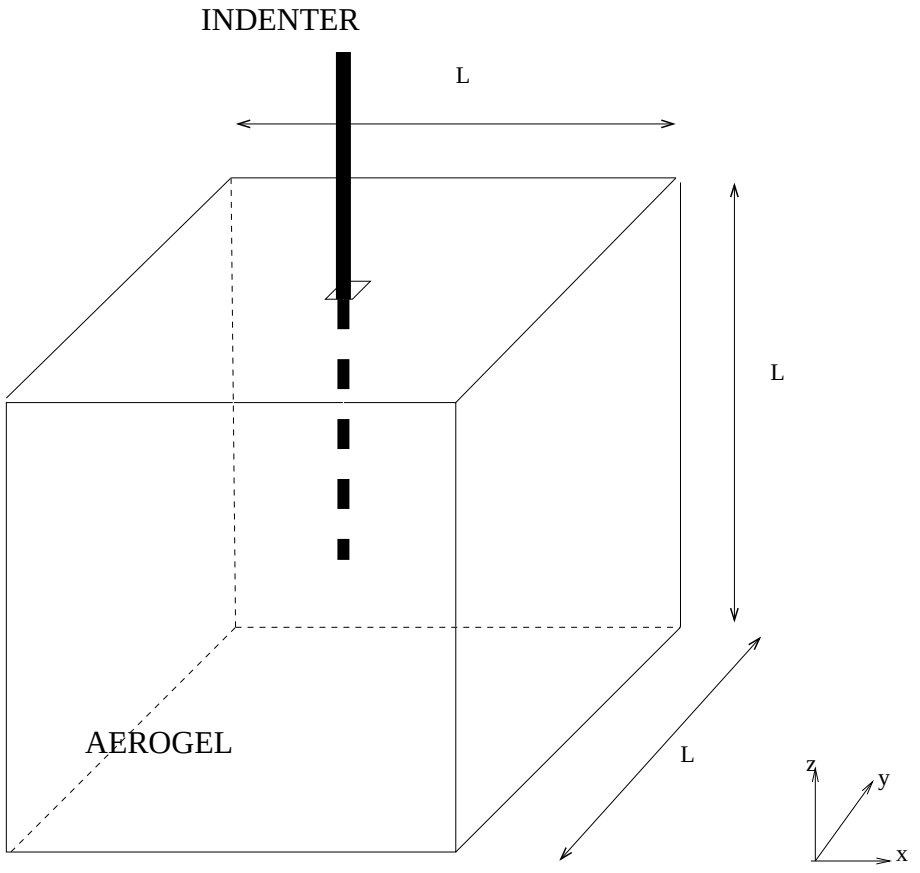

FIG. 1. Schema of the material and the indenter

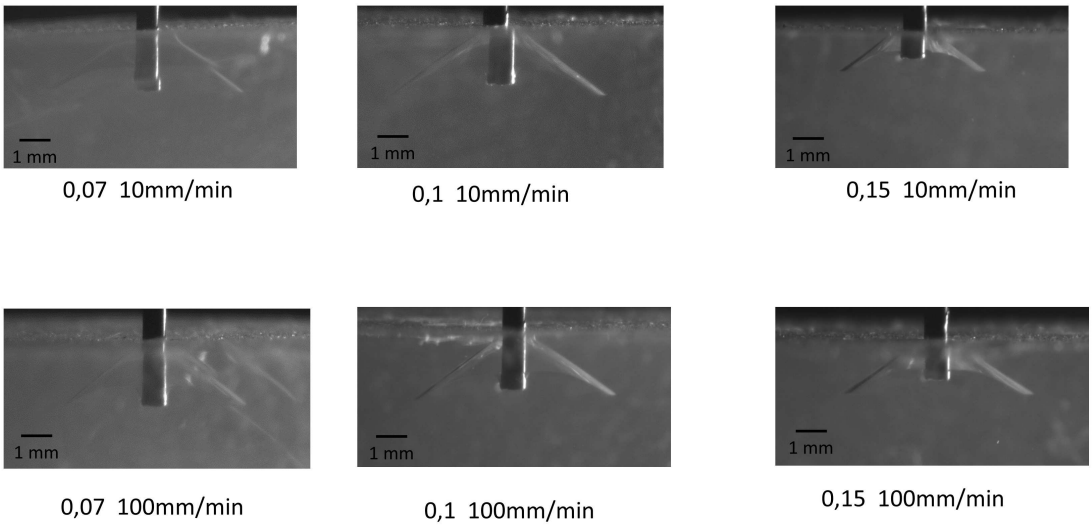

FIG. 2. Crack pictures in different aerogels for different densities and different indentation velocities.

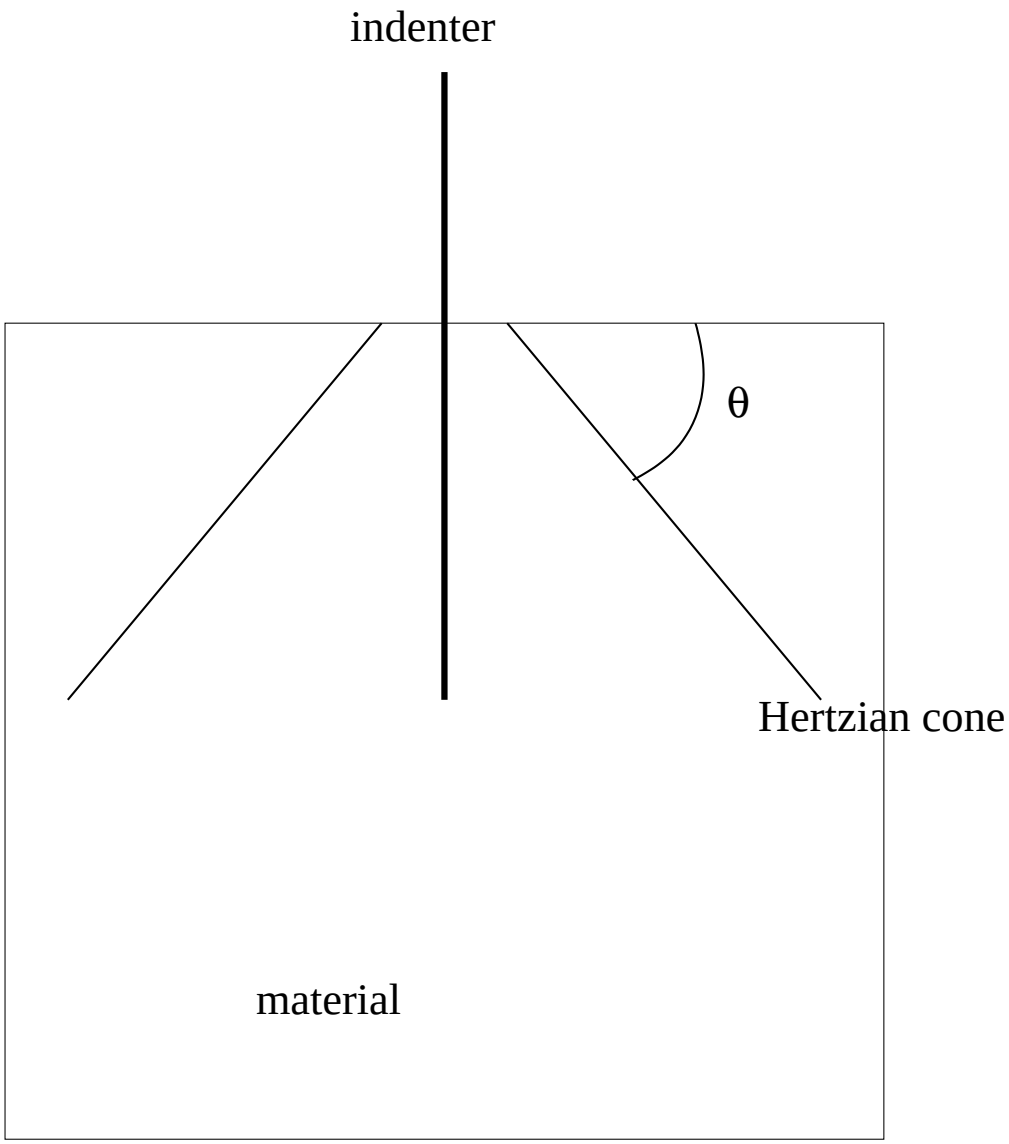

FIG. 3. Schema of the Hertzian cone angle θ

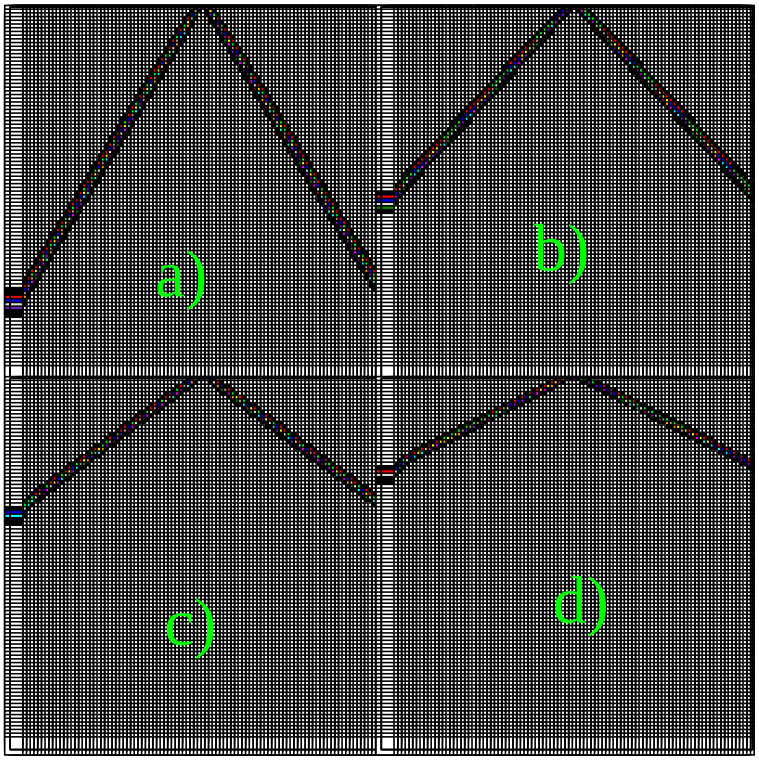

FIG. 4. Plot of the stresses for an indentation depth of $2A.U.$, the black squares represent the upper boundaries of the Hertzian cone crack due to the indenter (cut of the threedimensionnal fracture in the (y, z) plane) . The colored squares represent the stresses above the crack. The stress due to the indenter is equal to $10A.U.$. a) Poisson ratio $\nu = 0.15$; rupture threshold $500A.U.$; b) Poisson ratio $\nu = 0.2$; rupture threshold $500A.U.$;c) Poisson ratio $\nu = 0.25$; rupture threshold $500A.U.$;d)Poisson ratio $\nu = 0.3$; rupture threshold $500A.U.$

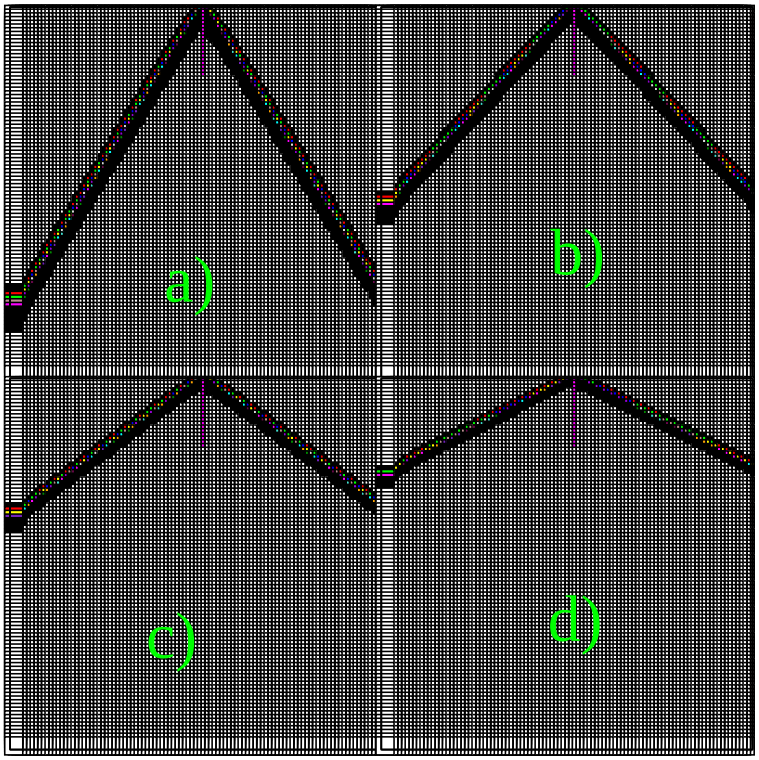

FIG. 5. Plot of the stresses for an indentation depth of $8A.U.$, the black squares represent the upper boundaries of the Hertzian cone crack due to the indenter (cut of the threedimensionnal fracture in the (y, z) plane). The colored squares represent the stresses above the crack. The stress due to the indenter is equal to $10A.U.$. a) Poisson ratio $\nu = 0.15$; rupture threshold $500A.U.$; b) Poisson ratio $\nu = 0.2$; rupture threshold $500A.U.$;c) Poisson ratio $\nu = 0.25$; rupture threshold $500A.U.$;d)Poisson ratio $\nu = 0.3$; rupture threshold $500A.U.$

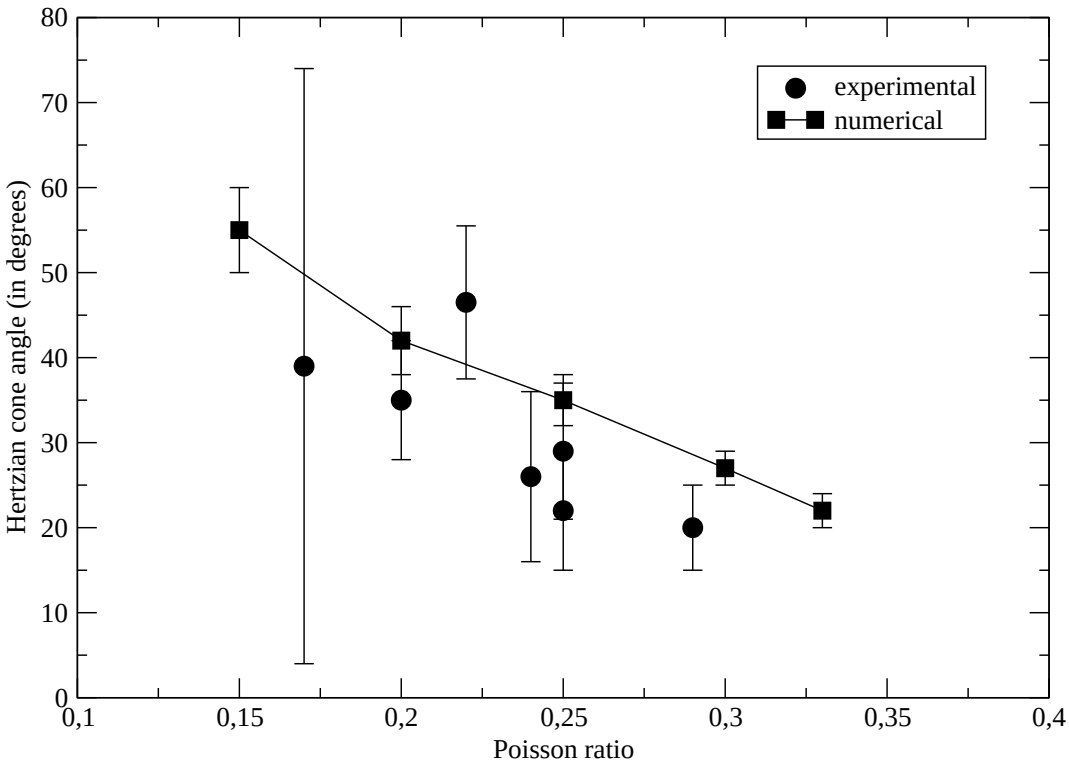

FIG. 6. Plot of the values of the Hertzian cone angle as a function of the Poisson ratio. Squares : numerical results. Circles: experimental results.